CHAPTER III

THE SIMULATION OF ONE LITHIUM ION IN LIQUID HYDROXYLAMINE

For this chapter, the first solvation structure for Li^+ in liquid hydroxylamine has been determined by using MC simulation method. An analytical intermolecular pair potential function Li^+-NH_2OH has been constructed on the basis of *ab inito* MO SCF calculations with ECP-DZP basis set. With this function, a Monte Carlo simulation for one lithium ion in 216 hydroxylamine molecules has been performed.

Methods

3.1 Intermolecular Potential Function

3.1.1 Performance of *ab initio* calculations

The DZP-ECP basis set for hydroxylamine was taken from a previous work [31], in which several basis sets had been tested critically for their ability to reflect the relative strength of all possible hydrogen bonds in dimer structures correctly, compared to near-HF-limit CEPA (Coupled Electron Pair Approximation) calculations (see Table 3.1). The NH_2OH-NH_2OH potential developed with this basis set has also been used successfully in MC simulations of the pure liquid hydroxylamine [32,33]. An analogous DZP-ECP basis set for Li^+ was taken from Steven *et al.*[22]. The ECP and atomic basis sets used during all SCF calculations are shown in Table 3.2 and 3.3, respectively. O and N basis sets were augmented by a d-type polarization function with orbital exponent 1.154 and 0.864, respectively [34]. The NH_2OH geometry used for this study was obtained by Tsunekawa [35], and was presented below this line

Bond Length (Å)	Bond Angle (degree)
O-H = 0.962	HNH = 107.1
N-O = 1.453	HON = 101.4
N-H = 1.017	HNO = 103.2

Table 3.1 NH_2OH geometry optimization for different basis set compare to experimental geometry**

Basis set	Bond Length (Å)			Bond Angle (degree)		Energy (Hartree)
	N-H	N-O	O-H	HNH	HON	
DZV*	1.000	1.431	0.952	111.9	107.0	-130.96
DZP*	1.002	1.400	0.943	107.3	104.6	-131.03
TZV*	0.999	1.430	0.951	111.5	104.3	-130.98
TZP*	0.999	1.399	0.940	107.6	104.8	-131.04
ECP/DZV*	1.004	1.434	0.956	111.6	106.6	-27.003
ECP/DZP*	1.005	1.406	0.946	106.9	104.5	-27.052
this work						
DZP	1.002	1.401	0.944	107.4	104.6	-131.03
					CPU =	2408
ECP/DZP	1.005	1.406	0.946	107.2	104.5	-27.052
					CPU =	409
CEPA*	1.017	1.453	0.960	105.2	101.8	-131.46
Expt.**	1.017	1.453	0.962	107.1	101.4	-

*and ** were taken from reference [31] and [35], respectively.

ศูนย์วิทยทรัพยากร
จุฬาลงกรณ์มหาวิทยาลัย

Table 3.2 Orbital-exponent Gaussian basis sets for atoms[22]

Atom	Function Type	α	Cs	Cp
Li	1s	0.61770	-0.16287	0.06205
		0.14340	0.12643	0.24719
		0.05048	0.76179	0.52140
	2s	0.01923	0.21800	0.34290
N	1sp	6.403	-0.13955	0.10336
		1.580	0.05492	0.33205
		0.5094	0.71678	0.48708
	2sp	0.1623	0.33210	0.31312
	d	0.864	1.0	
O	1sp	8.519	-0.14550	0.11007
		2.073	0.08286	0.34969
		0.6471	0.74325	0.48093
	2sp	0.2000	0.28472	0.30727
	d	1.154	1.0	
Cl	1s	2.225	-0.33098	
		1.173	0.11528	
	2s	0.3851	0.84717	
		0.1301	0.26534	
	2p	2.225	-0.12604	
		1.173	0.29952	
	3p	0.3851	0.58357	
		0.1301	0.34097	

ศูนย์วิทยทรัพยากร
จุฬาลงกรณ์มหาวิทยาลัย

Table 3.3 Effective core potential [22] for atoms dealing with this work

The form of the analytic representation is :

$$r^2V_l(r) = \sum_k A_{lk} r^{nlk} e^{-B_{lk}r^2}$$

Atom	ECP	A_{lk}	n_{lk}	B_{lk}
Li	V_p	-0.73963	1	1.34306
	V_{s-p}	1.80131	0	0.61284
		3.54971	2	1.64881
N	V_p	-0.91212	1	11.99686
	V_{s-p}	1.93565	0	3.83895
		21.73355	2	11.73247
O	V_p	-0.92550	1	16.11718
	V_{s-p}	1.96069	0	5.05348
		29.13442	2	15.95333
Cl	V_d	-3.40738	1	4.87483
	V_{s-d}	6.50966	0	17.00367
		42.27785	2	4.10380
	V_{p-d}	3.42860	0	8.90029
		22.15256	2	3.52648

First, two geometries of Li^+-NH_2OH complex (see Figure 3.1(a) and (b)) were optimized with this basis set, the results are collected in Table 3.4 and compared to the corresponding values for hydroxylamine itself. The difficulty to reproduce the experimental geometry of hydroxylamine by SCF calculations has been pointed out previously [31], and especially for a correct N-O bond length inclusion of correlation effects is inevitable.

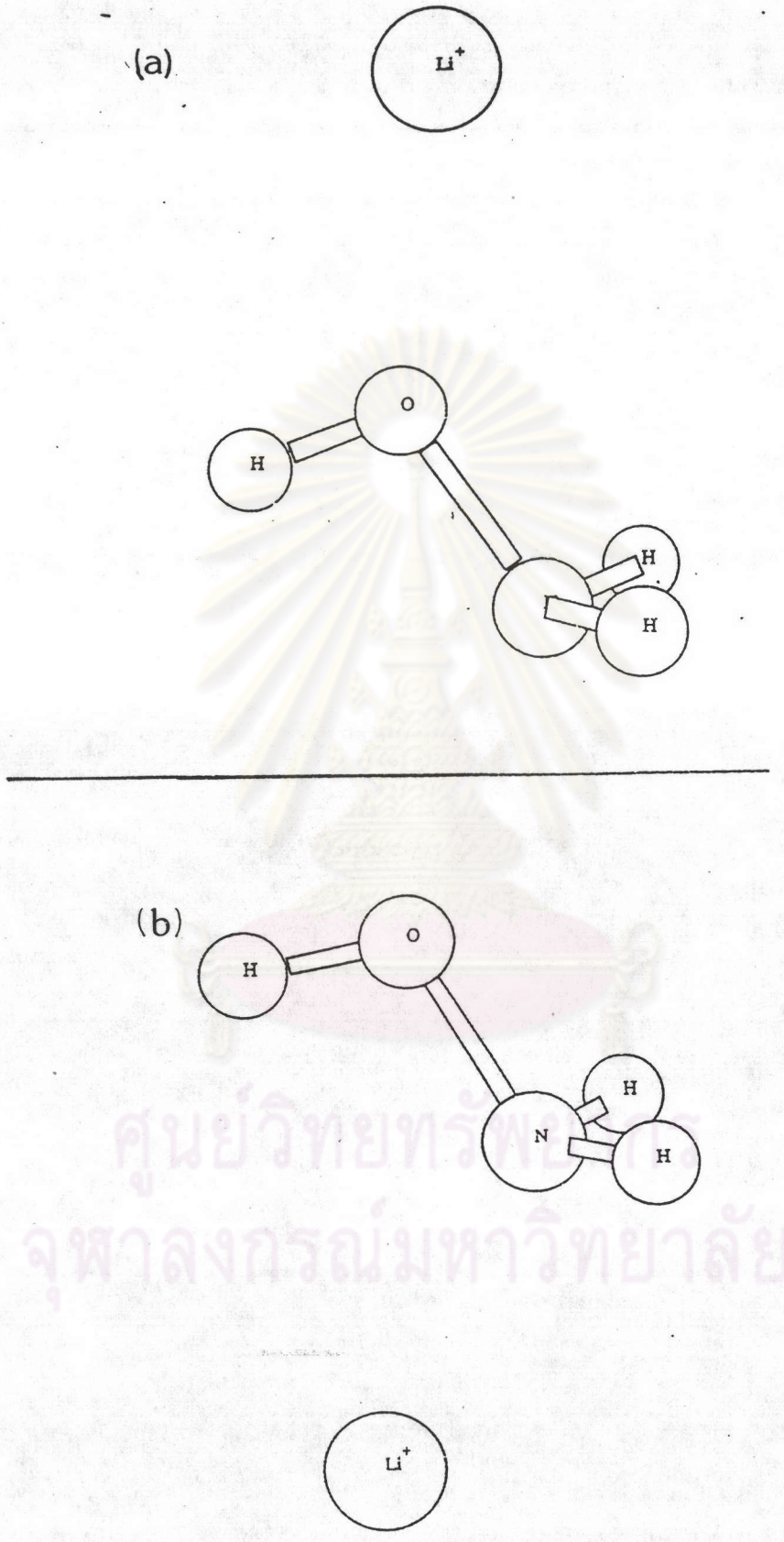

Figure 3.1 The optimized Li^+-NH_2OH geometries at position (a) and (b)

ศูนย์วิทยทรัพยากร
จุฬาลงกรณ์มหาวิทยาลัย

Table 3.4 Optimized geometrical parameters (in Å and Degree) for NH_2OH and Li^+-NH_2OH

N-H	N-O	O-H	Li-O	Li-N	NOH	E_{SCF} (Hartree)	Note
1.005	1.406	0.946	-	-	104.5	-27.052	ECP/DZP[31]
							this work
1.005	1.421	0.946	2.058	3.267	103.8	-27.0946	(a)
1.009	1.406	0.947	3.288	2.249	108.6	-27.0871	(b)
1.017	1.453	0.962	-	-	101.4	-	Expt. [35]

In that previous investigation, the used ECP-DZP basis set had proven to be a reasonable compromise between accuracy and computational effort, as the construction of a whole energy surface at the CEPA level would be prohibitively expensive in computer time. The comparison of the optimized geometrical parameters for NH_2OH and Li^+-NH_2OH obtained by this basis set shows that the changes induced in the molecule's internal geometry by Li^+ complex are not too large so that the experimental geometry of the isolated molecule could be used for the construction of the Li^+-NH_2OH energy surface.

In the global minimum (the lowest energy was found in this work), Li^+ is clearly coordinated to oxygen, as can be seen from the energy, the Li^+-O and Li^+-N distances (-27.0946 kcal/mol, 2.06 and 3.27 Å, respectively) in Table 3.4. It should be mentioned, however, that chelate coordinated structures do not differ too much in energy from this most stable arrangement.

i17396117

Some additional calculations have been performed in order to estimate the possible influence of basis set superposition errors, although it could be expected from previous investigations [31,32] that they should be small for the ECP-DZP basis set. For this purpose, several complex conformations at and near the global minimum of the energy surface and for some larger Li^+-O distances (up to 5 Å) were performed including the Boys-Bernardi counterpoise correction [24]. The result of this study can be summarized as following: the position of the global minimum is not shifted, the maximum superposition error around the global minimum is only 0.14 kcal/mole less than 1% of the minimum stabilization energy (-27.39 kcal/mole) and vanishes at ion-ligand distances above 3 Å. The applicability of the intermolecular potential obtained within this framework for MC/MD simulations seems to be granted; therefore, at least for studies on liquid structure and species distributions, whereas for the evaluation of sensitive thermodynamic or spectroscopic data empirical corrections of an employment of a considerably more sophisticated methodology (large all-electron basis set, flexible intramolecular geometry, correlation influence and 3-body terms) may be needed.

For the representation of the interaction energy surface, a lithium ion has been placed at numerous positions around hydroxylamine molecule by concerning with special regard to chemically representative conformations while a hydroxylamine molecule has been fixed during all calculations. With this selection, 358 *ab initio* energy points which correspond to the configuration mentioned in chapter II have been calculated in order to determine the Li^+-NH_2OH interaction energies used for fitting potential on the next step. Furthermore SCF points have been determined while testing the quality of the fitting to an analytical potential function (*vide infra*) so that the intermolecular potential function has been tested finally on the basis of 398 points of the energy surface.

ศูนย์วิทยทรัพยากร
จุฬาลงกรณ์มหาวิทยาลัย

3.1.2 Fitting of the Intermolecular Pair Potential

The interaction energies ΔE_{SCF} obtained by the *ab initio* calculations were fitted to an analytical potential of the form

$$\Delta E_{FIT} = \sum_{i=1}^{5} \frac{q_{Li} q_i}{r_{Li^+-i}} + \frac{A_{1i}}{r^m_{Li^+-i}} + \frac{A_{2i}}{r^n_{Li^+-i}} + A_{3i} \exp(-A_{4i} r_{Li^+-i}) \qquad (3.1)$$

where q denotes the partial charges of the atoms obtained by Mulliken population analysis [25], r_{Li^+-i} the distances between Li^+ and the i^{th} atom of hydroxylamine, and A_{1i}, A_{2i}, A_{3i} and A_{4i} the fitting parameters. For various values of n and m, fitting was performed by a non-linear Marquard-Levenberg algorithm [27], minimizing the squared differences between fitted and SCF ΔE values. Weight factors were introduced to give special emphasis to values near the global and local energy minima, values above 30 kcal/mole were excluded. The best resulting funotion was tested according to the procedure of Beveridge *et al.* [28], through which additional SCF points were included in the fitting procedure until the standard deviation remained constant and sufficiently small.

3.2 Monte Carlo Simulation

A simulation was carried out by the programme MC91 [36] for a system consisting of one Li^+ ion and 216 NH_2OH molecules at 305 K. Corresponding to the density of pure hydroxylamine of 1.204 $g.cm^{-3}$ at this temperature, the elementary box length was set to be 21.436 Å, and half of this distance was chosen as cut-off radius for exponential terms. The starting configuration was chosen randomly, and equilibration was achieved after 1 million configurations. Other two million configurations were used for sampling and analyzing the data to evaluate the characteristic values(*eg.* RDFs and integration number *etc.*).

ศูนย์วิทยทรัพยากร
จุฬาลงกรณ์มหาวิทยาลัย

Results and Discussion

3.3 Potential Function

The best fit of the analytical function outlined in the previous topic obtained were

$$\Delta E_{FIT} = \sum_{i}^{5} \frac{q_{Li^+} q_i}{r_{Li^+-i}} + \frac{A_{1i}}{r^4_{Li^+-i}} + \frac{A_{2i}}{r^7_{Li^+-i}} + A_{3i}\exp(-A_{4i} r_{Li^+-i}) \qquad (3.2)$$

The value of m and n are 4 and 7, respectively. The standard deviation obtained was less than 10 % of the lowest stabilization energy (-27.39 kcal/mol) which is in the acceptable limit. The atomic charge and the final fitting parameters of the function are given in Table 3.5 and 3.6, respectively. The SCF calculated and potential fitted energy curves are shown in Figure 3.2. The comparison of interaction energies: potential fitted values versus *ab initio* calculated for all studied points is presented in Figure 3.3.

ศูนย์วิทยทรัพยากร
จุฬาลงกรณ์มหาวิทยาลัย

Table 3.5 Fractional atomic charges , where H_N and H_O are hydrogen atoms bonded to N and O atoms, respectively.

Atom	Charge (atomic unit)
Li^+	+1.0
N	-0.482
H_N	+0.301
O	-0.525
H_O	+0.405

Table 3.6 Final fitting parameters of Li^+-NH_2OH pair potential function

Pair	A_1 (kcal.Å^4. mol^{-1})	A_2 (kcal.Å^7. mol^{-1})	A_3 (kcal. mol^{-1})	A_4 (Å^{-1})
Li^+-H_N	-294.882	499.368	377.458	1.266
Li^+-N	-2490.941	4743.527	6580.365	2.145
Li^+-O	438.151	-7202.369	553645.735	4.829
Li^+-H_O	-659.565	1160.711	690.983	1.472

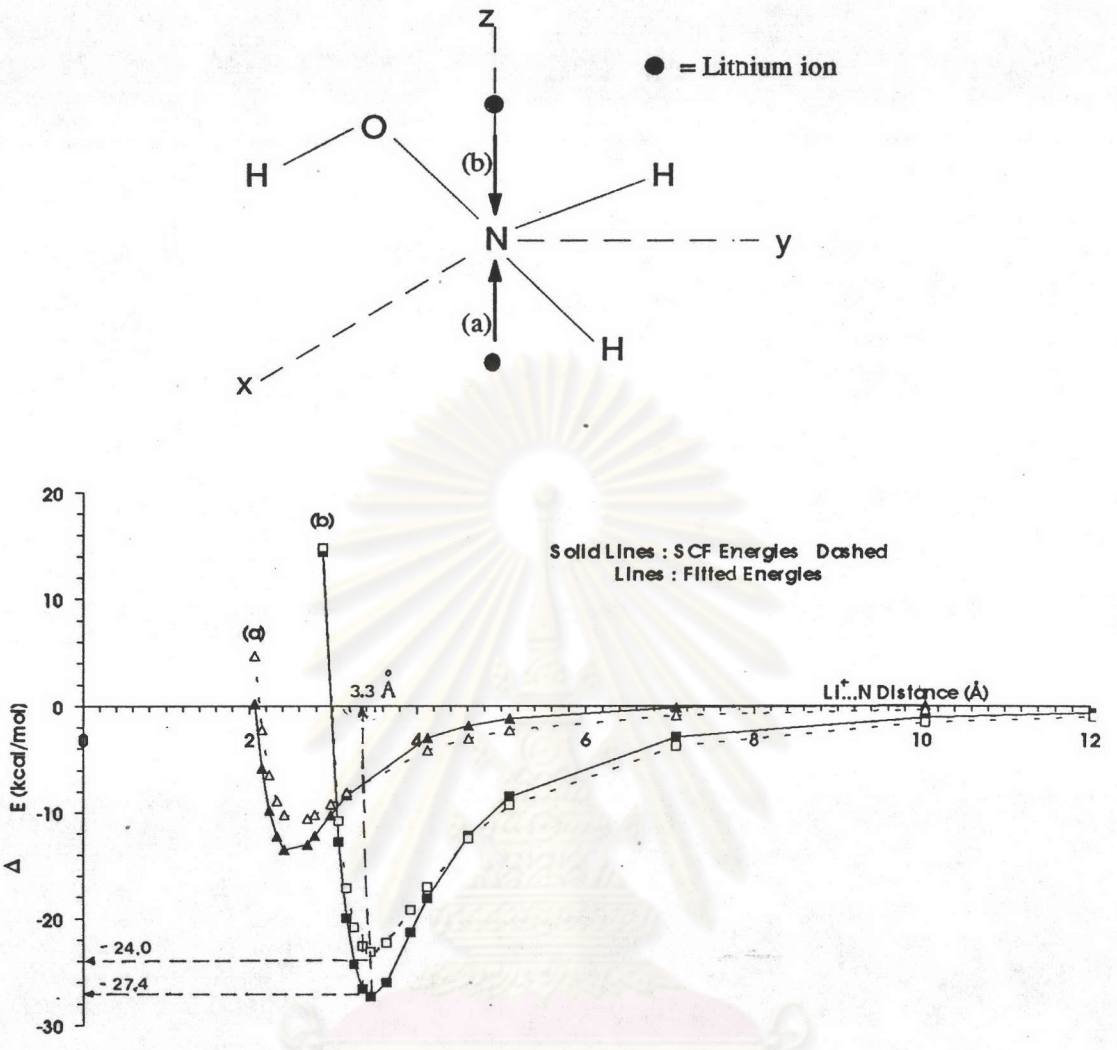

Figure 3.2 Comparison between ab initio SCF calculated and potential fitted energy curves for Li^+-NH_2OH according to (a) and (b) directions

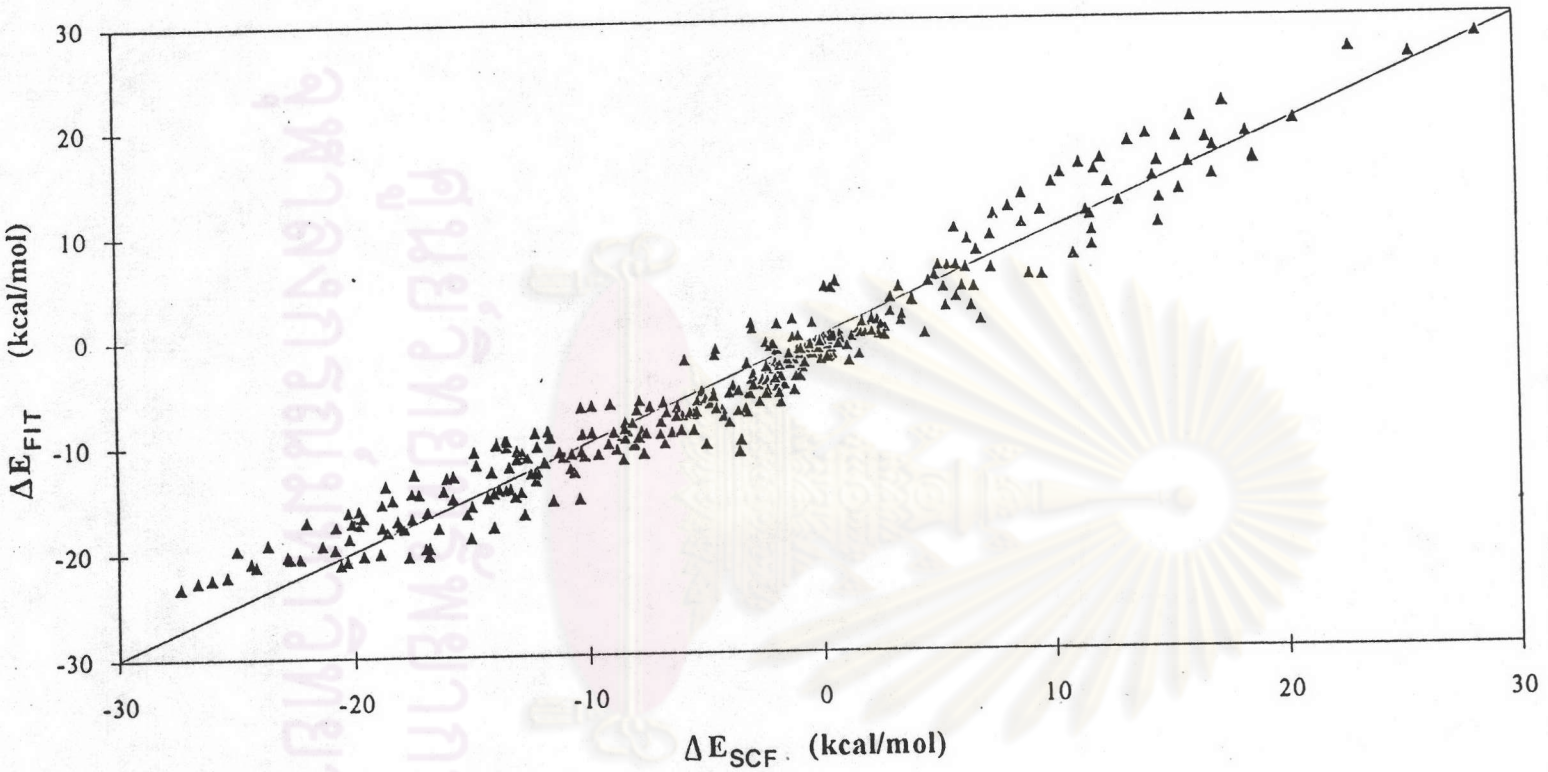

Figure 3.3 Comparison of interaction energies: potential fitted values versus *ab initio* SCF calculated for all points in the set.

3.4 Solvation structure of Li^+-NH_2OH system

The structure of the solvent is apparently not influenced to a recognizable extent by the ion. All characteristic data of the radial distribution functions (RDFs) and pair energy distribution are identical to those reported in [32-33]. RDFs of the solvent for the present work are reported in Appendix VII

The RDFs for Li^+-O and Li^+-N are shown in Figure 3.4, together with their running integration, the characteristic data of these and the Li^+-H RDFs are collected in Table 3.7. The RDFs clearly reveal that the orientation of NH_2OH molecules in the first solvation sphere is not uniform: two of the ligands give a first maximum in the Li^+-N RDF at 2.2 Å, whereas 5 others are represented by a second peak of this RDF centered around 3.3 Å. The Li^+-O RDF shows two closely neighboring peaks at 2.0 and 2.3 Å, and their integration corresponds to 5 for the first and 2 further ligand molecules for the second peak. This finding allows the following interpretation: two of the ligands in the first solvation shell are chelate-coordinated via both N and O of one and the same NH_2OH molecule, and other 5 molecules are coordinated only via the oxygen site. The Li^+-H RDFs reveal that this coordination leads to a rather unfavorable location for the H_O, quite close to the cation. This location does not allow much variation so that all 7 H atoms are found in one very sharp peak. The Li^+-H_N RDF, on the other hand, distinguishes between the ligands in chelate coordination and the others: for the former, a peak is found between 2.6 and 3.2 Å. the other 5 are found between 3.2 and 4.2 Å. The RDF data indicate that the optimal Li^+-NH_2OH solvate structure, although apparently a "*compromise arrangement*", should be rather rigid and not allow an easy exchange of the coordinated ligands.

ศูนย์วิทยทรัพยากร
จุฬาลงกรณ์มหาวิทยาลัย

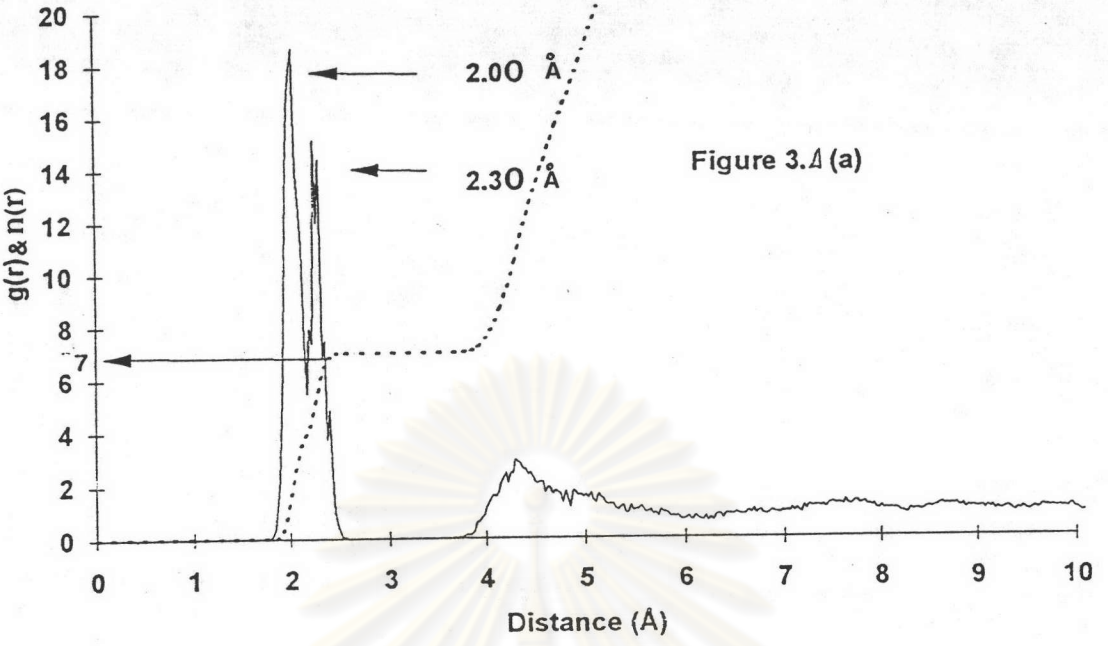

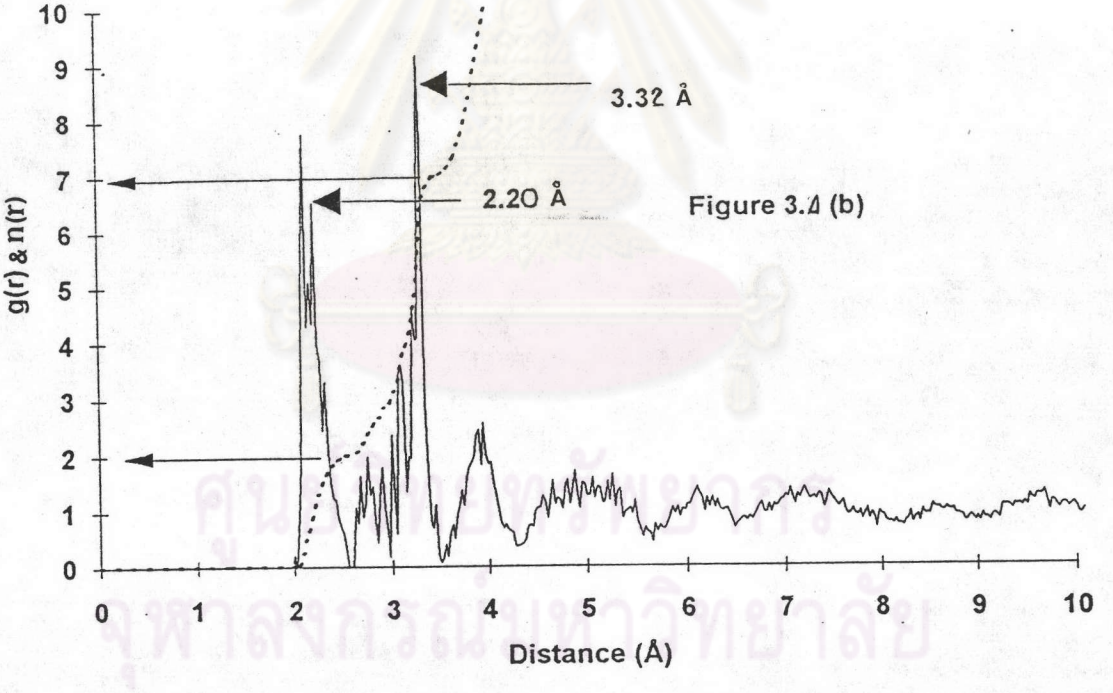

Figure 3.4 Radial distribution functions for Li^+-O(a), Li^+-N(b), Li^+-H_O(c) and Li^+-H_N(d) and its integration (dotted line)

Figure 3.4 (continue)

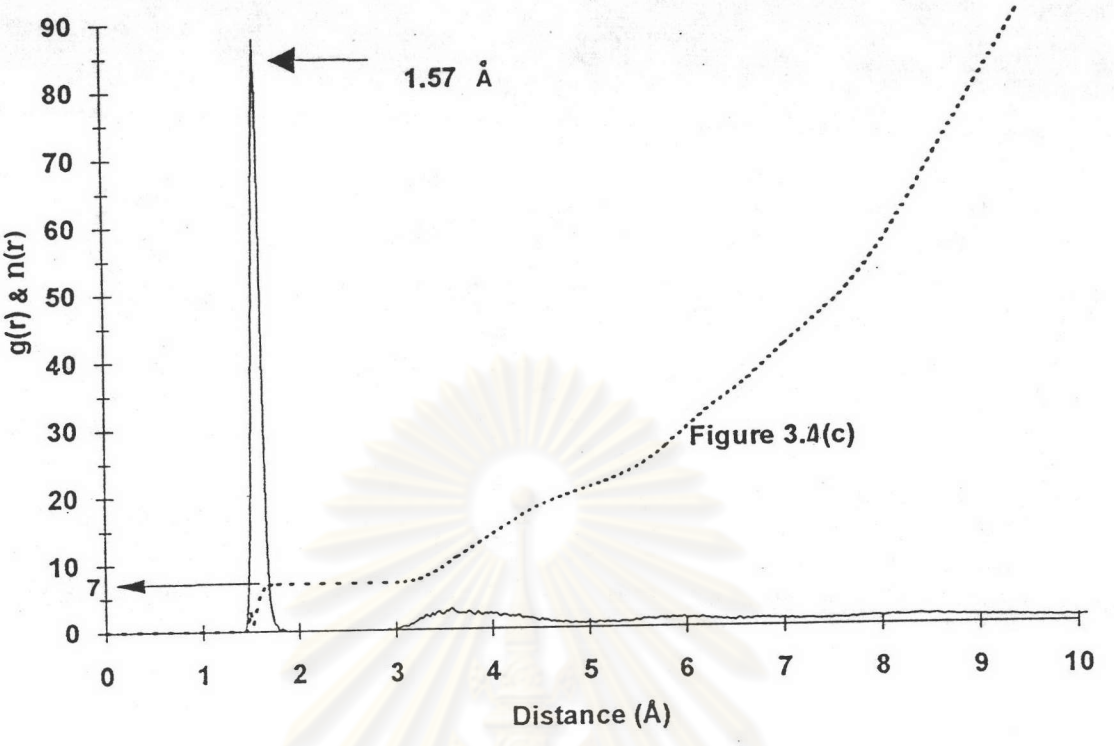

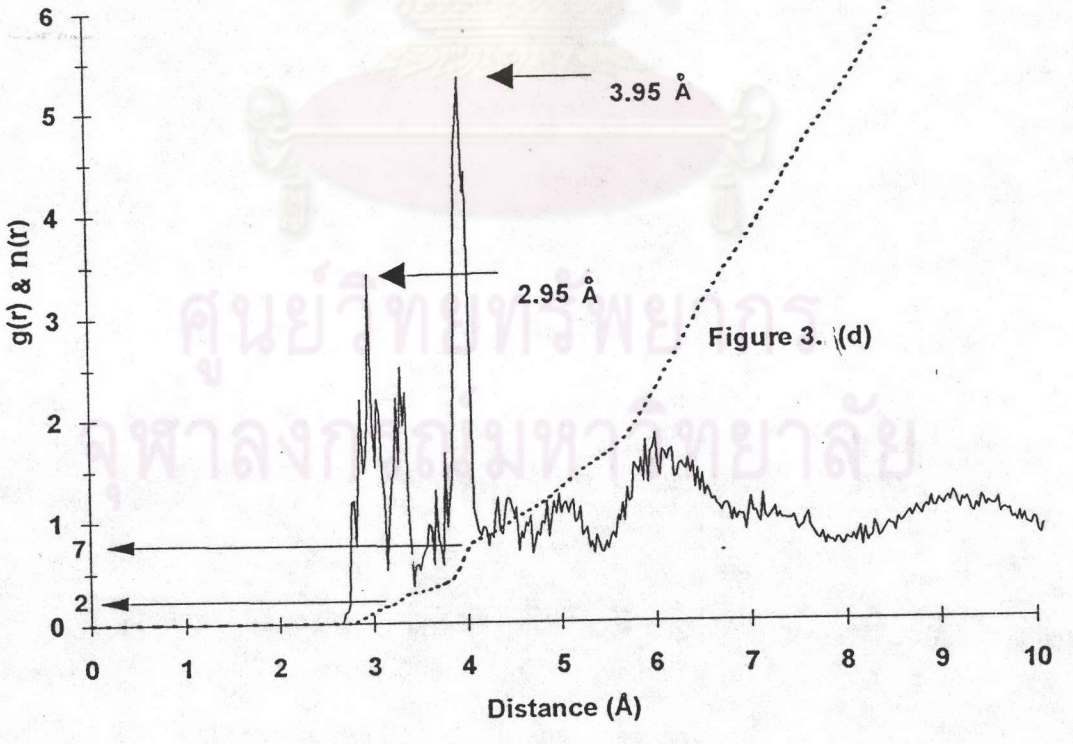

ศูนย์วิทยทรัพยากร
จุฬาลงกรณ์มหาวิทยาลัย

Table 3.7 Characteristic values of Li^+ RDFs (first coordination shell)

RDF	r_{max}	r_{min}	n
Li-O*	2.00	2.18 (5.0)**	5.0
	2.30	2.57 (0.0)**	2.0
Li-N*	2.20	2.60 (0.0)**	2.0
	3.32	3.52 (0.0)**	5.0
Li-H_O	1.57	1.80	7.0
Li-H_N*	2.95	3.20 (0.5)**	2.0
	3.95	4.20 (0.8)**	5.0

r_{max} denotes RDF maxima, r_{min}, RDF minima, and n, the integration value up to r_{min}

* split peak, ** height of the peak

A second shell can be recognized between ~4 and ~6 Å, and in this shell nitrogen atoms are closer to the central ion than oxygens, probably due to O-H...N hydrogen bonding, which was found to be the strongest one in NH_2OH dimers [31].

A detailed analysis of the simulation's history files leads to the coordination number distributions based on the molecule's center of mass location presented in Figure 3.5: if one extends the search to a sphere of 4.5 Å around the ion, which would correspond to the Li-N RDF minimum where a separation of the first shell with its sharp peaks from the more diffuse second shell can be assumed, it reveals that the coordination number of 7 is rather exclusive for the first shell, with only minor contributions of 8- and 6-coordinated species. Therefore the previous interpretation given on the basis of both RDFs, indicating 2 chelate- and 5 O-coordinated ligands in the ion surrounding, appears confirmed as the appropriate description of the first shell.

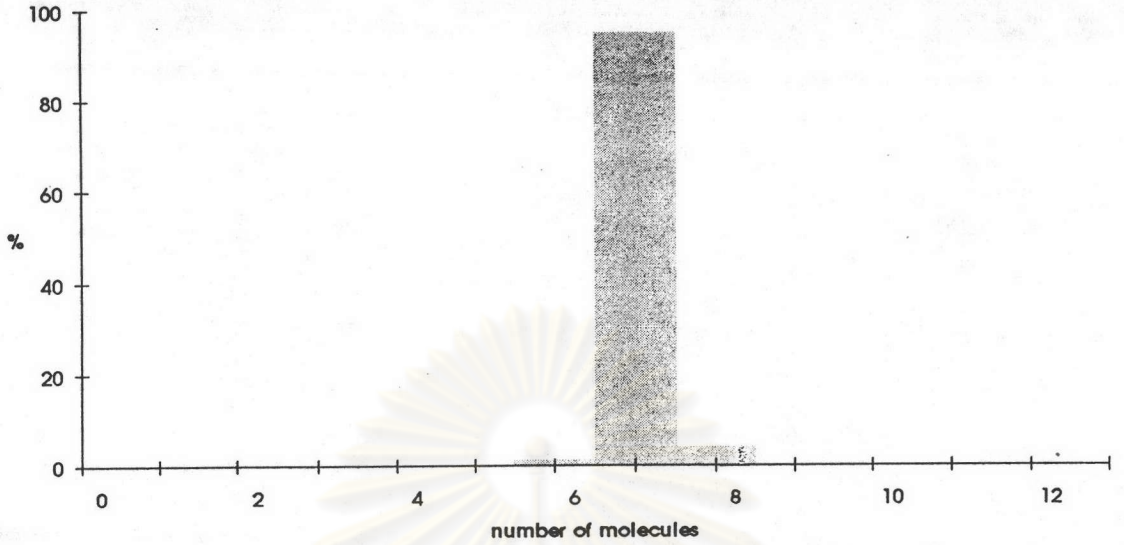

Figure 3.5 Coordination number distribution for Li^+-NH_2OH center of mass (first shell, up to 4.5 Å)

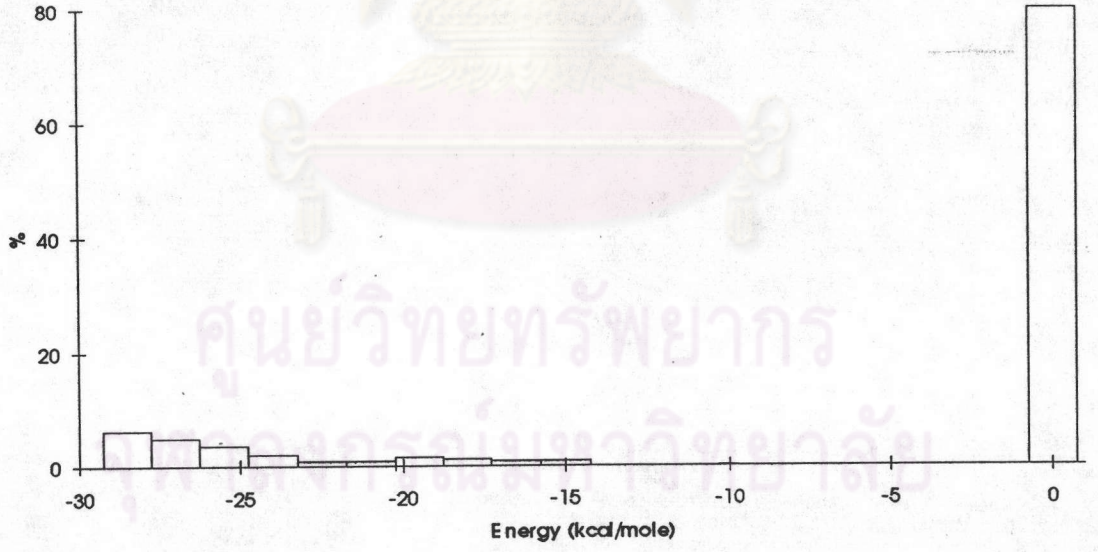

Figure 3.6 Pair energy distribution for Li^+-NH_2OH center of mass considering all NH_2OH molecules around the ion

The pair energy distribution for Li^+-NH_2OH is shown in Figure 3.6. It shows that the first shell ligands bind with 20 - 30 kcal/mole to the ion, whereas the large majority of ligands located at more distant positions interacts only weakly with the central ion. The "*second*" shell therefore appears more as a structural entity formed around the first-shell solvate, shaped mainly by hydrogen bonding with the first-shell ligands but not so much through ion influence. Nevertheless, the total solvation energy of the Li^+ ion, defined as the sum of interactions with all hydroxylamine molecules, still amounts to ~650 kcal/mole.

To compare the results of this study, the position of the first maxima and the corresponding-running integration numbers for the first solvation shell in water, ammonia, water/ammonia mixture, methylamine and hydroxylamine are presented in Table 3.8. It is also satisfying to note that in this work the average distance of Li^+-O and Li^+-N is in good agreement with the former reports [7, 8, 38-41] both computer simulation and experimental (x-ray) study. However, one uncertainty remaining in the interpretation of the results of this simulation can be seen in Table 3.8 with the higher coordination number due to the possible of excluding the influence of 3-body effects. Although these effects do not alter significantly the structure of hydrated Li^+, there are some indications that this may not be true for Zn^{2+} in water and ammonia [9, 10]. On the other hand, interaction energies are not very high and equilibrium distances between ion and ligand quite "*reasonable*" in the case of hydroxylamine. This, together with the larger size of the ligand allows the assumption that the structures found in this work should be reliable. A final decision in this matter would, however, imply the construction of a 3-body correction function, which is connected with an enormous effort in compution of at least 1000 NH_2OH ..Li^+ ..NH_2OH clusters in all varieties of geometrical arrangement, and thus beyond the scope of this study.

ศูนย์วิทยทรัพยากร
จุฬาลงกรณ์มหาวิทยาลัย

Table 3.8 Comparison of characteristic values of RDFs for Li^+ in various solvents.

Sovent	Method	Atom	r_{max}	n
H_2O	MC [38]	O	2.10	6.0
	MD [39]	O	1.98	5.3
	x-ray [40]	O	1.97	5.8
NH_3	MD [41]	N	2.05	4.0
	MD [7]	N	2.01	6.0
H_2O+NH_3	MC [8]	N	2.50	2.0
		O	1.95	4.0
CH_3NH_2	MD [41]	N	1.97	4.0
NH_2OH	MC (this work)	N	2.20	7.0
		O	2.00	7.0

Another possible error source is the use of rigid ligand molecules in the simulations. The unfavourable location of OH hydrogens in the first solvation shell could possibly be improved by a model allowing intramolecular relaxation, and also this effect seems worthwile further investigation.

ศูนย์วิทยทรัพยากร
จุฬาลงกรณ์มหาวิทยาลัย